



Short-to-medium range structure and glass-forming ability in metallic glasses

Guanying Wei ¹, Junzhi Cui,^{1,2} Wei Wang,¹ Xiaoxiang Guo,¹ Jingli Ren ^{1,*} and Weihua Wang^{3,*}

¹Henan Academy of Big Data, Zhengzhou University, Zhengzhou 450052, China

²Institute of Computational Mathematics, Chinese Academy of Sciences, Beijing 100190, China

³Institute of Physics, Chinese Academy of Sciences, Beijing 100190, China



(Received 30 June 2021; accepted 10 May 2022; published 31 May 2022)

In this paper, we investigate the clustering model and glass-forming ability (GFA) in response to variant compositions and cooling rates. The structural units are obtained by molecular dynamics and hierarchical clustering. In the clustering model, a nesting relationship from small- to large-scale units, i.e., from short- to medium-range order, is observed during the hierarchical clustering. Furthermore, the packing efficiency of short-range units is applied to depict the GFA, and the result suggests that the packing efficiency is not strictly increased with respect to cooling rate. A positive correlation between a high packing efficiency and a large skewness is found, which validates that alloys with the stronger GFA have a more disordered structure.

DOI: [10.1103/PhysRevMaterials.6.055601](https://doi.org/10.1103/PhysRevMaterials.6.055601)

I. INTRODUCTION

The atomic structure of metallic glasses (MGs) is a formidable scientific challenge in condensed matter physics. Unlike metallic crystals, MGs have no long-range translational or orientational order, although some degrees of short- and medium-range order do exist [1]. Initially, the local units in MGs were supposed to have the same type of structure as their crystalline compounds with similar composition in the stereochemically defined model [2,3]. This model is still controversial, as the experimental evidence has not been conclusive. Solute-centered clusters were identified as the fundamental building blocks or short-range order in MGs [4–6]. Taking the earlier models further, the idealized cluster packing schemes, such as efficient cluster packing on a cubic lattice [4] and quasi-equivalent clusters on an icosahedral packing [5], were proposed and provided insights on the medium-range order in MGs. Recently, a local $SU(2)$ bonding topology depicted the connectivity rules in the model of binary glasses [7] based on the local bonding constraints developed by Nelson [8]. These structural motifs play an important role in understanding the structure of MGs. Here, we propose innovative structural motifs containing one, two, and three coordination layers to study the structural model about the MGs.

Indirect criteria to estimate glass-forming ability (GFA) have been proposed [9,10], including the critical cooling rate [11], width of subcooled liquid zone [12,13], and reduced glass transition temperature [14]. Li *et al.* [15] discovered a universal indicator Δq , i.e., the width of the first peak in x-ray diffraction (XRD), for depicting GFA. Additionally, numerous investigators suggest that glass formation of an alloy is affected by short-range order and its interconnectivity [16,17]. It was perceived that the structures of MGs could contain partial crystalline orders [18], and the hidden orders

were formulated by inheriting the order of the crystal during glass formation [19]. The formation of hidden orders during cooling and their topological entanglement produced geometric frustration against crystallization, which correlated closely with the GFA [19]. From a short-range perspective, the higher atomic packing efficiency resulted in stronger glass formation [20,21]. There was also a correlation between medium-range structure and glass formation in Zr-Cu-Al MGs, and the results suggested that improving GFA in this alloy system may depend more on destabilizing crystallike structures than enhancing noncrystalline structures [22].

How to depict the short-range order to long-range disorder in MGs has remained an open problem. Motivated by this issue, we propose a structural model of MG by molecular dynamics and hierarchical clustering (a kind of method in machine learning). Here, we choose the binary Cu-Zr MG as a representative material because it has a broad composition region forming MG ribbons [23] and a relatively simple system [24]. Initially, we use molecular dynamics simulation to get the atomic coordination of CuZr MGs, then structural units are obtained directly from the atomic position without human intervention. A clustering model is proposed according to the nesting relation of structural units. In addition, the packing efficiency of the structural motifs is utilized to investigate the effects of alloy composition, cooling rate, and structural order on GFA.

II. METHODS

A. Preparation of Cu-Zr MGs

The initial B2 Cu-Zr alloy is enlarged by $20 \times 20 \times 20$, $50 \times 50 \times 50$, and $100 \times 100 \times 100$ to construct $\text{Cu}_{50}\text{Zr}_{50}$ MGs containing 16 000, 250 000, and 2 000 000 atoms, respectively. The Cu and Zr atoms account for half each. Based on the embedded atom method potential [25], the periodic boundary condition is applied to simulate in three Cartesian

*renjl@zzu.edu.cn; whw@iphy.ac.cn

directions. Relaxing the system 2 ns under the isothermal-isobaric (NPT) ensemble, the initial temperature of the system is 2798 K, and the pressure is 0 GPa. A time step of 2 fs is used. The system is cooled down continuously to 298 K at the rate of 20 K/ps and relaxed for 2 ns to obtain the stable amorphous state. For the $\text{Cu}_{50}\text{Zr}_{50}$ alloy containing 16 000 atoms, $\text{Cu}_{50}\text{Zr}_{50}$ MGs are obtained at cooling rates of 10^{11} , 10^{12} , 10^{13} , and 10^{14} K/s of different orders of magnitude and rates of 5×10^{12} , 8×10^{12} , 5×10^{13} , and 8×10^{13} K/s of different values of the same order of magnitude. Moreover, we randomly substitute an appropriate number of Cu atoms with the same number of Zr atoms in the initial alloy ($\text{Cu}_{50}\text{Zr}_{50}$ alloys with 16 000 atoms) to obtain $\text{Cu}_{40}\text{Zr}_{60}$, $\text{Cu}_{64}\text{Zr}_{36}$, and $\text{Cu}_{80}\text{Zr}_{20}$ alloys. The corresponding MGs are obtained by the same rapid cooling method. They are applied to investigate the impact of composition on GFA.

B. Structural units obtained by hierarchical clustering

Hierarchical clustering is the most common unsupervised machine learning method to find natural groupings and patterns in data [26]. The hierarchical clustering algorithm can be further classified into agglomerative method and divisive method according to whether the hierarchical decomposition is formed bottom up or top down. Here, we adopt the agglomerative method. Specifically, Statistic and Machine Toolbox [27,28] functions including *pdist*, *linkage*, and *cluster* perform all the necessary steps. Firstly, the similarity between every pair of atoms should be recognized. The *pdist* function is used to determine the Euclidean distance between every pair of atoms. Secondly, the atoms are grouped into a binary, hierarchical dendrogram. The *linkage* function is applied to determine how atoms should be divided into clusters according to the proximity between atoms in the dataset. As data points are paired into binary clusters, the newly formed clusters are grouped into larger clusters until a hierarchical dendrogram is determined. Thirdly, the *cluster* function, $T = \text{cluster}(X, \text{maxclust}, m)$ is used to create clusters by detecting natural groupings in the hierarchical dendrogram X . Here, m is the number of categories into which the clustering dendrogram is finally divided, but it is not a certain number. It is determined by the number of times required to filter out all structural units that meet the conditions (the number of atoms in the structural unit is less than or equal to the truncation parameter) under the selected truncation parameter currently. The truncation parameter is chosen as the number of atoms in the short- and medium-range structural units. See also the Supplemental Material [29] for the pseudocode of hierarchical clustering.

We want to get the structural units of different scales (with different coordination layers). Short-range order refers to the nearest-neighbor atomic environment, and medium-range order refers to the second or third nearest-neighbor arrangement [30]. From the atomic-pair distribution function $g(r)$ in Fig. 1, $\text{Cu}_{50}\text{Zr}_{50}$ MG has obvious first and second peaks and weak third peaks due to structural characteristics. The cutoff distance of first, second, and third neighbors r_1 , r_2 , and r_3 are selected, respectively, and we can get structural units with the first, second, and third layer coordination numbers n_1 , n_2 , and

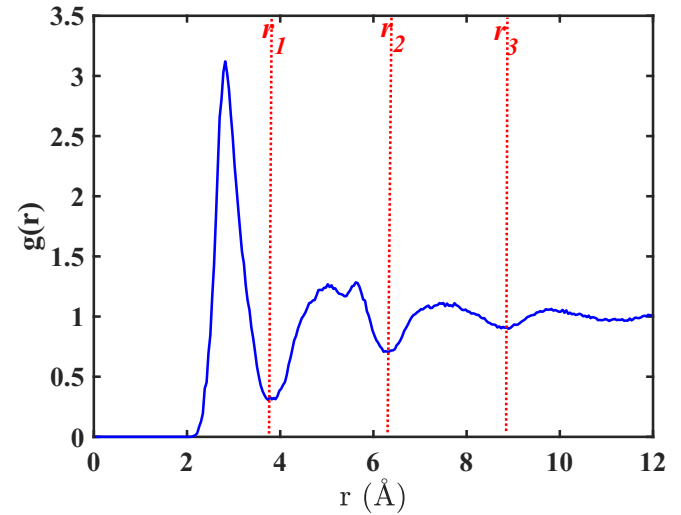


FIG. 1. Atomic-pair distribution function $g(r)$ of $\text{Cu}_{50}\text{Zr}_{50}$ metallic glass and the cutoff distance r_1 , r_2 , and r_3 .

n_3 , respectively, combined with Eq. (1):

$$n = 4\pi\rho \int_0^{r_0} r^2 g(r) dr, \quad (1)$$

where n is the coordination number corresponding to the radial distance r_0 , and ρ is the number density. Here, $n_1 + 1$, $n_2 + 1$, and $n_3 + 1$ are selected as truncation parameters, respectively. Taking truncation parameter $n_1 + 1$ as an example, the specific clustering process is as follows. Beginning with $m = 1$, m is incremented by 1. All the effective structural units (i.e., the atomic number in structural units is less than or equal to $n_1 + 1$) will be recorded under $m = N$ (N is a positive integer). Then $m = N + 1$, the qualified structural units that have no intersection with the previously recorded results are recorded. The clustering process ends when all atoms are grouped into effective structural units. The clustering process with $n_2 + 1$ and $n_3 + 1$ as truncation parameters is similar. In this way, we apply hierarchical clustering to the whole $\text{Cu}_{50}\text{Zr}_{50}$ MG to obtain the short- and medium-range structural units.

Moreover, according to Miracle's efficient cluster packing model [4,31], the nearest coordination number of the central solute atom of the cluster is calculated by Eq. (2) but not in the average sense:

$$N^T = \begin{cases} \frac{4\pi}{6\arccos\left\{\sin\left(\frac{\pi}{3}\right)\left[1 - \frac{1}{(\tilde{R}+1)^2}\right]^{1/2}\right\} - \pi}, & 0.225 \leq \tilde{R} < 0.414, \\ \frac{4\pi}{8\arccos\left\{\sin\left(\frac{\pi}{4}\right)\left[1 - \frac{1}{(\tilde{R}+1)^2}\right]^{1/2}\right\} - 2\pi}, & 0.414 \leq \tilde{R} < 0.902, \\ \frac{4\pi}{10\arccos\left\{\sin\left(\frac{\pi}{5}\right)\left[1 - \frac{1}{(\tilde{R}+1)^2}\right]^{1/2}\right\} - 3\pi}, & 0.902 \leq \tilde{R} < \infty, \end{cases} \quad (2)$$

where N^T represents the coordination number of the solute atom in the first coordination shell, and \tilde{R} is the ratio of the atomic radius at the center of the cluster to the radius of coordination atom. This N^T also can be selected as the truncation parameter to get the structural units that only have the nearest coordinate layer. Then the packing efficiency of structural units is calculated to explore GFA.

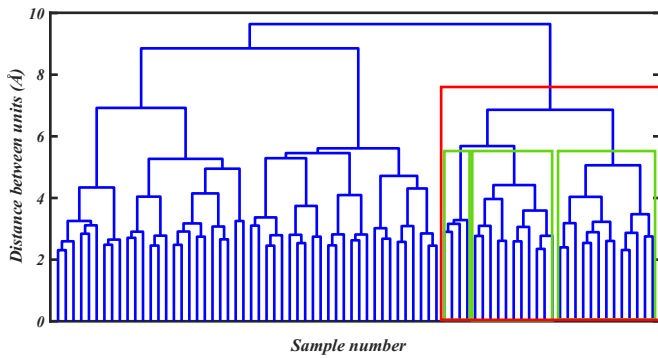


FIG. 2. The nested relationships of structural units with different scales in hierarchical clustering. The three green rectangles frame three structural units with one coordination layer, the red rectangle frames a structural unit with two coordination layers, and the whole hierarchy dendrogram is a structural unit with three coordination layers.

III. RESULTS AND DISCUSSION

A. Clustering model

How the short-range ordered structure is stacked into the long-range amorphous structure is still a difficult problem. Some existing structural models show how short-range units form medium-range units [4,5]. Based on the idea of hierarchical clustering, we explore how short-range units stack up to form long-range structures in MG. Bernal's random dense packing of hard spheres shows two structural characteristics of MGs: random and dense-packed [32]. Hierarchical clustering classifies units according to their similarity. When the similarity is measured by the distance between the atoms, the atoms in similar structural units are very close to each other, and such structural units can be understood as dense structures. Combining with the truncation parameters $n_1 + 1$, $n_2 + 1$, and $n_3 + 1$, hierarchical clustering is applied to the coordinate data of MGs to obtain the dense structure with different scales.

How these close-packed structures form the whole structure is worth discussing. We take $\text{Cu}_{50}\text{Zr}_{50}$ MG as an example to explore its structure. Utilizing $n_1 + 1 = 14$ as the truncation parameter, the structural units are in small sizes and are located at the bottom of the hierarchical dendrogram. With the increasing truncation parameter, the distribution level of the obtained structural units in the hierarchical dendrogram is also improved. Figure 2 displays the nesting of units in the clustering process. The hierarchical dendrograms surrounded by three green rectangles represent the typical structural units with $n_1 + 1$ as the truncation parameter, and the hierarchical dendrogram surrounded by the red rectangle represents the typical structural unit with $n_2 + 1$ as the truncation parameter. A whole tree is a unit including 78 atoms with $n_3 + 1$ as the truncation parameter. In $\text{Cu}_{50}\text{Zr}_{50}$ MG, structural units of different scales are divided under different truncation parameters. In the atomic coordinates of structural units obtained by large truncation parameters, the atomic coordinates of structural units with small scale as truncation parameters are found, that is, small-scale units are nested in large-scale units. Figure 3 shows the nesting relationship of structural units with different scales. In state I, red, yellow, and blue spherical

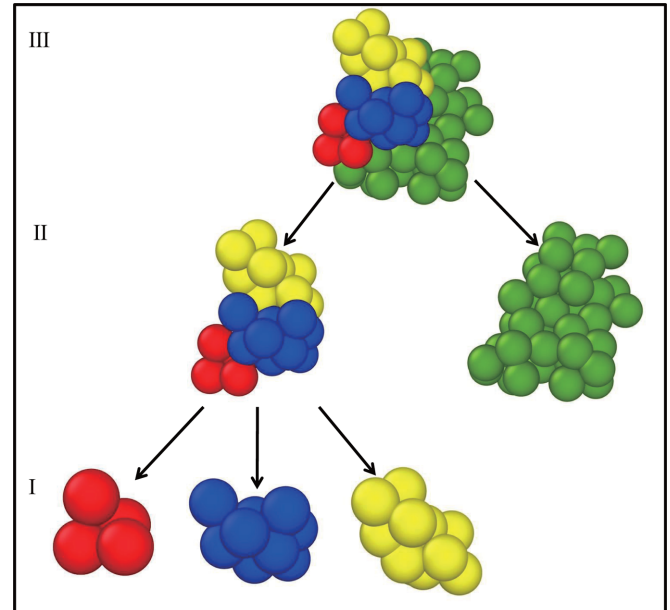


FIG. 3. The nested relationships among structural units with one, two, and three coordination layers. State I is three units with one coordination layer obtained when the truncation parameter is $n_1 + 1$. Then these three units are clustered into effective structural units with two coordination layers in state II due to the small Euclidean distance. The unit with three coordination layers in state III is clustered by the two nearest units with two coordination layers in state II.

units represent three short-range units. These three short-range structural units together constitute the medium-range unit with $n_2 + 1$ as the truncation parameter in state II. In the same way, mesoscale structure units are nested within a large-scale unit in state III.

It is a necessary condition for the model to be established that the atom-pair distribution function $g(r)$ of the model agrees with the experimental results. The $g(r)$ of the structural units with one, two, and three coordination layers are calculated. The $g(r)$ is a discrete histogram because of the fewer atoms in structural units. Results show that the fitting curves $g(r)$ of structural units containing one, two, and three coordination layers in Figs. 4(a), 4(b), and 4(c) are like the curves about the first peak, the first two peaks, and the first three peaks of total atomic-pair distribution function $g(r)$ in Fig. 1. The process of hierarchical clustering can reveal the formation process of MG from short to long range. We define this structural model of MGs connected by clustering trees as a clustering model.

B. Atomic-scale mechanisms of the GFA

The dense packing principle may be the key factor for GFA [33]. The higher the packing efficiency, the stronger the GFA [21]. The N^T in Eq. (2) is used as the truncation parameter to obtain dense structural units. According to the measured data of Egami and Waseda [34], a Cu atom has a radius of 0.127 nm, and a Zr atom has a radius of 0.158 nm. If the Cu atom is the central atom, according to Eq. (2), the nearest coordination numbers are from 10 to 13. Similarly, the nearest coordination numbers for the Zr atom are from

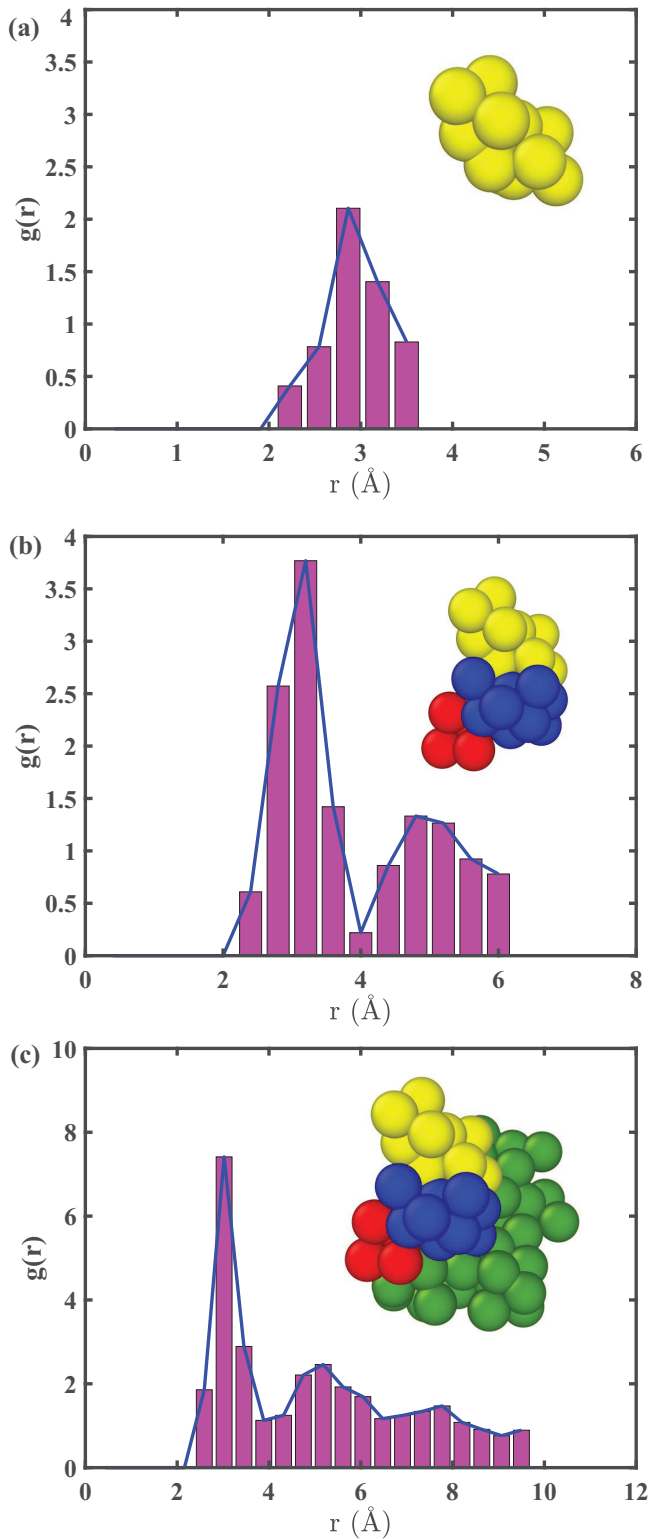


FIG. 4. Structural units and the corresponding atomic-pair distribution functions for the (a) small scale, (b) medium scale, and (c) large scale.

13 to 17. Therefore, we select 18 (the maximum number of atoms in a cluster containing a layer of coordination atoms) as the truncation parameter of hierarchical clustering. In this way, the number of atoms in the effective structural units is

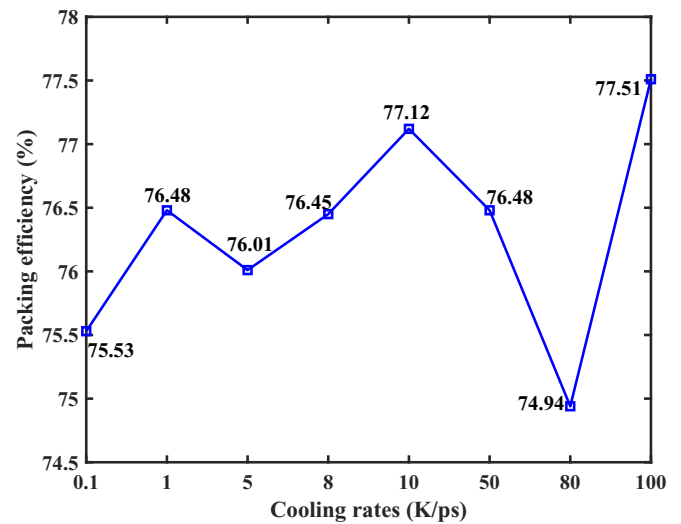


FIG. 5. The average of packing efficiency about $\text{Cu}_{50}\text{Zr}_{50}$ metallic glasses in five simulations under different cooling rates.

≤ 18 . We divide the effective structural unit into tetrahedral sets by Delaunay triangulation [35,36]. The packing efficiency of each structural unit is the sum of the packing efficiency of the tetrahedron, which is the sum of the atomic volumes in the tetrahedron divided by the volume of the tetrahedron. The packing efficiency of the whole MG is the weighted average of the packing efficiency of structural units. See also the Supplemental Material [29] for the specific calculation of packing efficiency. The effect of different compositions and cooling rates on the GFA are investigated by the packing efficiency.

We calculate the packing efficiency of $\text{Cu}_{50}\text{Zr}_{50}$ MG under different cooling rates and the packing efficiency of $\text{Cu}_{40}\text{Zr}_{60}$, $\text{Cu}_{50}\text{Zr}_{50}$, $\text{Cu}_{64}\text{Zr}_{36}$, and $\text{Cu}_{80}\text{Zr}_{20}$ MGs. We do the simulation five times for each chosen cooling rate with different initial temperature seeds. The average packing efficiency under different cooling rates is displayed in Fig. 5. Usually, the faster the cooling rate, the higher the glass transition temperature T_g , and the easier the glass is to form [37]. For a finer division on cooling rate, the GFA does not increase strictly monotonically with increasing cooling rate. Under the cooling rates of 5×10^{12} and 8×10^{12} K/s between 1×10^{12} and 1×10^{13} K/s, the GFA fluctuates with the cooling rate. Similarly, under the cooling rates of 5×10^{13} and 8×10^{13} K/s between 1×10^{13} and 1×10^{14} K/s, the GFA is still not strictly increasing. This reveals that the effect of the cooling rate on glass formation is complex, and different structural realizations are possible during the process of cooling. Through calculating the packing efficiency of Cu-Zr MGs with different compositions, we discover that $\text{Cu}_{50}\text{Zr}_{50}$ MG has the highest packing efficiency, while $\text{Cu}_{64}\text{Zr}_{36}$ MG has relatively higher packing efficiency. The result is displayed in Fig. 6. This is consistent with the fact that $\text{Cu}_{50}\text{Zr}_{50}$ and $\text{Cu}_{64}\text{Zr}_{36}$ alloys have stronger GFAs [21,38].

Recently, Li *et al.* [15] proposed a Δq -GFA positive correlation criterion based on material genes, where Δq is the width of the first peak of XRD. A larger Δq indicates a shorter correlation length, and thus, an ordered arrangement of structural units can only be retained over a small distance, indicating

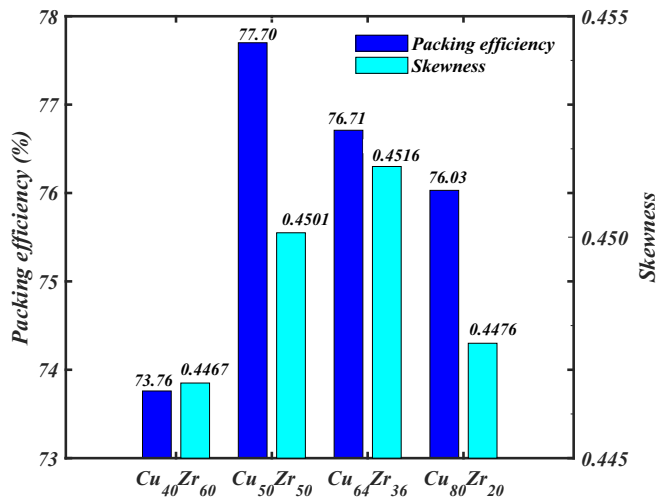


FIG. 6. The packing efficiency and skewness of Cu-Zr metallic glasses (MGs) with different compositions. Cu₅₀Zr₅₀ and Cu₆₄Zr₃₆ MGs have a high packing efficiency, strong glass-forming ability, and disordered structure.

that the amorphous structure is statistically more disordered. Here, we also illustrate the relationship between the degree of order and GFA in MGs with the help of statistical skewness γ describing the degree of symmetry, which does not depend on the experimental measurement of Δq . Skewness is a digital characteristic of the degree of asymmetry of statistical data distribution. See also the Supplemental Material [29] for the definition and general calculation of skewness. There is local symmetry in MGs because of the short-range order [39]. The skewness of structural units with one coordination layer in Cu₄₀Zr₆₀, Cu₅₀Zr₅₀, Cu₆₄Zr₃₆, and Cu₈₀Zr₂₀ MGs is calculated to reflect the degree of symmetry, and then the degree of order is described. Following, we give the specific calculation about the skewness. Skewness γ of a Cu-Zr MG

is the weighted average value of the skewness of the unit containing a coordination layer γ_i : $\gamma = \sum_{m=1}^M \gamma_i$, where M is the number of units containing a coordination layer in a MG. The skewness of each structural unit containing a coordination layer γ_i is the root mean square of the square sum of the skewness of each x , y , and z direction in the structural unit: $\gamma_i = \sqrt{(\gamma_x^2 + \gamma_y^2 + \gamma_z^2)}$. The value of skewness reflects the deviation of the atomic position from the central point. The larger the value of skewness, the lower the symmetry of structural units and the more the disorder in structural units. Cu₅₀Zr₅₀ and Cu₆₄Zr₃₆ MGs have a larger skewness among the Cu-Zr binary glasses, and the result is displayed in Fig. 6. The variation trends of skewness and packing efficiency of MGs with different components are consistent. This also validates that alloys with strong GFA have a more disordered structure.

IV. CONCLUSIONS

Combing molecular dynamics simulation with hierarchical clustering, we obtain the structural units at different scales without interference. In the clustering process, we observe a nesting relationship from small- to large-scale units and propose a clustering model. Moreover, the packing efficiency of structural units implies that Cu₅₀Zr₅₀ alloy has a stronger GFA, and the impact of the cooling rate on glass formation is not strictly monotonous. The Cu-Zr alloy with a higher packing efficiency has a larger skewness, indicating that the alloy with a stronger GFA has a more disordered structure.

ACKNOWLEDGMENT

This paper is supported by the National Natural Science Foundation of China (No. 52071298) and ZhongYuan Science and Technology Innovation Leadership Program (No. 214200510010).

- [1] D. B. Miracle, *Acta Mater.* **54**, 4317 (2006).
- [2] P. H. Gaskell, *Nature (London)* **276**, 484 (1978).
- [3] P. H. Gaskell, *J. Non-Cryst. Solids* **32**, 207 (1979).
- [4] D. B. Miracle, *Nat. Mater.* **3**, 697 (2004).
- [5] H. W. Sheng, W. K. Luo, F. M. Alamgir, J. M. Bai, and E. Ma, *Nature (London)* **439**, 419 (2006).
- [6] D. Ma, A. D. Stoica, L. Yang, X. L. Wang, Z. P. Lu, and J. Neufeind, *Appl. Phys. Lett.* **90**, 211908 (2007).
- [7] P. M. Derlet, *Phys. Rev. Materials* **4**, 125601 (2020).
- [8] D. R. Nelson, *Phys. Rev. B* **28**, 5515 (1983).
- [9] Z. P. Lu and C. T. Liu, *Phys. Rev. Lett.* **91**, 115505 (2003).
- [10] S. Guo, Z. P. Lu, and C. T. Liu, *Intermetallics* **18**, 883 (2010).
- [11] W. H. Wang, C. Dong, and C. H. Shek, *Mater. Sci. Eng., R* **44**, 45 (2004).
- [12] A. Inoue and T. Zhang, *J. Non-Cryst. Solids* **250-252**, 552 (1999).
- [13] J. Ding, Y. Q. Cheng, and E. Ma, *Acta Mater.* **69**, 343 (2014).
- [14] Z. P. Lu, H. Tan, Y. Li, and S. C. Ng, *Scr. Mater.* **42**, 667 (2000).
- [15] M. X. Li, Y. T. Sun, C. Wang, L. W. Hu, S. Sohn, J. Schroers, W. H. Wang, and Y. H. Liu, *Nat. Mater.* **21**, 165 (2022).
- [16] N. Jakse and A. Pasturel, *Appl. Phys. Lett.* **93**, 113104 (2008).
- [17] Y. Q. Cheng, E. Ma, and H. W. Sheng, *Phys. Rev. Lett.* **102**, 245501 (2009).
- [18] H. Tanaka, T. Kawasaki, H. Shintani, and K. Watanabe, *Nat. Mater.* **9**, 324 (2010).
- [19] Z. W. Wu, M. Z. Li, W. H. Wang, and K. X. Liu, *Nat. Commun.* **6**, 6035 (2015).
- [20] Y. Li, Q. Guo, J. A. Kalb, and C. V. Thompson, *Science* **322**, 1816 (2008).
- [21] L. Yang, G. Q. Guo, L. Y. Chen, C. L. Huang, T. Ge, D. Chen, P. K. Liaw, K. Saksl, Y. Ren, Q. S. Zeng, B. LaQua, F. G. Chen, and J. Z. Jiang, *Phys. Rev. Lett.* **109**, 105502 (2012).
- [22] P. Zhang, J. J. Maldonis, M. F. Besser, M. J. Kramer, and P. M. Voyles, *Acta Mater.* **109**, 103 (2016).
- [23] A. Inoue, C. Suryanarayana, and T. Masumoto, *J. Mater. Sci.* **16**, 1391 (1981).
- [24] X. D. Wang, S. Yin, Q. P. Cao, J. Z. Jiang, H. Franz, and Z. H. Jin, *Appl. Phys. Lett.* **92**, 011902 (2008).
- [25] M. I. Mendelev, D. J. Sordelet, and M. J. Kramer, *J. Appl. Phys.* **102**, 043501 (2007).

- [26] W. H. E. Day and H. Edelsbrunner, *J. Classif.* **1**, 7 (1984).
- [27] A. K. Jain and R. C. Dubes, *Algorithms for Clustering Data* (Prentice-Hall, Upper Saddle River, NJ, 1988).
- [28] M. H. Yang, J. H. Li, and B. X. Liu, *J. Alloys Compd.* **757**, 228 (2018).
- [29] See Supplemental Material at <http://link.aps.org/supplemental/10.1103/PhysRevMaterials.6.055601> for the pseudocode of hierarchical clustering, the clustering results, and the calculation of skewness.
- [30] X. X. Yue, A. Inoue, C.-T. Liu, and C. Fan, *Mater. Res.* **20**, 326 (2017).
- [31] D. B. Miracle and W. S. Sanders, *Philos. Mag.* **83**, 2409 (2003).
- [32] J. D. Bernal, *Nature (London)* **185**, 68 (1960).
- [33] K. Zhang, W. W. Smith, M. L. Wang, Y. H. Liu, J. Schroers, M. D. Shattuck, and C. S. O'Hern, *Phys. Rev. E* **90**, 032311 (2014).
- [34] T. Egami and Y. Waseda, *J. Non-Cryst. Solids* **64**, 113 (1984).
- [35] P. Su and R. L. S. Drysdale, *Comput. Geom.* **7**, 361 (1997).
- [36] D. Schwarzenbach, *Crystallography* (John Wiley and Sons, Chichester, 1996).
- [37] Y. Q. Cheng and E. Ma, *Prog. Mater. Sci.* **56**, 379 (2011).
- [38] K. N. Lad, *J. Non-Cryst. Solids* **404**, 55 (2014).
- [39] X. K. Xi, L. L. Li, B. Zhang, W. H. Wang, and Y. Wu, *Phys. Rev. Lett.* **99**, 095501 (2007).